Title:

Liver haploinsufficiency of RuvBL1 causes hepatic insulin resistance and enhances hepatocellular carcinoma progression.

Authors:

Tommaso Mello*[, 1], Maria Materozzi[1, §], Francesca Zanieri[1, §], Irene Simeone[1], Elisabetta Ceni[1], Oxana Bereshchenko[2], Simone Polvani[1], Mirko Tarocchi[1], Giada Marroncini[1], Claus Nerlov[3], Daniele Guasti[4], Daniele Bani[4], Massimo Pinzani[5], Andrea Galli[1].

Affiliations:

[1]Dept. of Experimental and Clinical Biomedical Sciences "Mario Serio", University of Florence, Florence Italy.

[2]Faculty of Medicine, University of Perugia, Perugia, Italy.

[3]MRC Molecular Hematology Unit, Weatherall Institute of Molecular Medicine, Radcliffe Department of Medicine, University of Oxford.

[4]Dept. of Clinical and Experimental Medicine, University of Florence, Florence, Italy.

[5]UCL Institute for Liver and Digestive Health, London, UK

Corresponding Author: *Tommaso Mello - email: tommaso.mello@unifi.it

List of abbreviations

This article has been accepted for publication and undergone full peer review but has not been through the copyediting, typesetting, pagination and proofreading process which may lead to differences between this version and the Version of Record. Please cite this article as doi: 10.1002/ijc. 32787

RuvBL1: Rvb-like 1; snRNP: small nucleolar RiboNucleoProteis; mTOR: mammalian Target Of Rapamycin; DEN: diethylnitrosamine; PCNA: Proliferating Cell Nuclear Antigen; HGF: Hepatocyte growth factor; TGFβ: Transforming growth factor beta; BrdU: Bromodeoxy-Uridine; OGTT: oral glucose tolerance test; PTT: pyruvate tolerance test, ITT: insulin tolerance test; PPAR: peroxisome proliferator-activated receptor; LXR: liver X receptor; SREBP: sterol regulatory element-binding protein

Electronic world count: 4315

Figures and tables: 6 main figures, 6 supplemental figures, 4 supplemental tables

Novelty and Impact

RuvBL1 is a multifaced protein overexpressed in hepatocellular carcinoma (HCC) and a potential target for anti-cancer strategy. However, whether RuvBL1 actively participates in the onset and progression of HCC remains elusive. We addressed this question subjecting conditional RuvBL1$^{hep+/-}$ mice to chemically-induced hepatic carcinogenesis. We found that RuvBL1 lies at the crossroad between hepatic glucose metabolism and cellular proliferation and that its targeting results in hyperglycemia and insulin resistance, promoting - rather than preventing - HCC development.

ABSTRACT

RuvBL1 is an AAA+ ATPase whose expression in hepatocellular carcinoma (HCC) correlates with a poor prognosis. In vitro models suggest that targeting RuvBL1 could be an effective strategy against HCC. However, the role of RuvBL1 in the onset and progression of HCC is still unknown. To address this question, we developed a RuvBL1$^{hep+/-}$ mouse model and evaluated the outcome of DEN–induced liver carcinogenesis up to 12 months of progression. We found that RuvBL1 haploinsufficiency initially delayed the onset of liver cancer, due to a reduced hepatocyte turnover in RuvBL1$^{hep+/-}$ mice. However, RuvBL1$^{hep+/-}$ mice eventually developed HCC nodules that, with aging, grew larger than in the control mice. Moreover, RuvBL1$^{hep+/-}$ mice developed hepatic insulin resistance and impaired glucose homeostasis. We could determine that RuvBL1 regulates insulin signaling through the Akt/mTOR pathway in liver physiology *in vivo* as well as in normal hepatocytic and HCC cell *in vitro*. Whole transcriptome analysis of mice livers confirmed the major role of RuvBL1 in the regulation of hepatic glucose metabolism. Finally, RuvBL1 expression was found significantly correlated to glucose metabolism and mTOR signaling by bioinformatic analysis of human HCC sample from the publicly available TGCA database. These data uncover a role of RuvBL1 at the intersection of liver metabolism, hepatocyte proliferation and HCC development, providing a molecular rationale for its overexpression in liver cancer.

KEYWORDS

Pontin; mTOR; Akt; glucose metabolism; cancer

INTRODUCTION

Hepatocellular carcinoma (HCC) is the fifth most common cancer in men and the second most common cause of cancer-related deaths worldwide[1]. Its mortality rate reaches 95% of incidence, reflecting the aggressive nature of this cancer and the limited availability of effective therapeutic options. A better understanding of HCC biology is therefore a pre-requisite to future development of more effective anti-cancer strategies. The highly conserved AAA+ ATPase RuvBL1 (Pontin52, TIP49a) is involved in key cellular processes such as chromatin remodeling, DNA repair, telomere maintenance, gene expression, snRNP assembly, mitosis, cell migration and invasion[2,3]. RuvBL1 also participates in p53, mTOR, c-myc and β-catenin intracellular signalling[2,3]. Its expression is upregulated in several human cancers, including HCC[4], and often correlates with a more aggressive cancer type. RuvBL1 inhibition effectively reduces the *in vitro* growth rate of HCC[4,5], leukemia[6] and lung[7] cancer cell lines, making this protein a potential target for anti-cancer strategy. Despite these promising results, it is still uncertain whether RuvBL1 plays any active role in the oncogenic transformation to HCC and in its progression. Moreover, the molecular mechanisms regulated by RuvBL1 both in the context of HCC and in the normal liver are largely unknown. Since systemic deletion of RuvBL1 is lethal[8], to address these questions we developed an hepatocyte-conditional hemizygous mouse model (RuvBL1$^{hep+/-}$), and monitored diethylnitrosamine (DEN)-induced liver cancer progression after 3, 6, 9 and 12 months. We found that the haploinsufficiency of RuvBL1 *per se* affects the regenerative potential of the liver and significantly delays the onset of DEN-induced liver cancer. However, it also seriously unbalances liver metabolism, leading to hyperglycemia and hepatic insulin resistance. Despite the initial delay, after 9-12 months of progression HCC nodules grew significantly larger in the RuvBL1$^{hep+/-}$ than in control mice. Finally, we have shown that RuvBL1

haploinsufficiency affects insulin signaling through the Akt/mTOR pathway, providing novel molecular clues on RuvBL1 functions at the intersection between liver metabolism and HCC development.

Materials and Methods

Cell culture

AML-12 cells were obtained from LGC Standards (Cat# CRL-2254, RRID:CVCL_0140) and maintained in DMEM/F12 (Carlo Erba, Italy) supplemented with 10% FBS (PAA Laboratories), ITS (Sigma-Aldrich), 40ng/ml dexamethasone (Sigma-Aldrich). Hepa1-6 cells were purchased from LGC Standards (Cat# CRL-1830, RRID:CVCL_0327) and maintained in DMEM (Gibco, Cat#41965) supplemented with 10% FBS. The HepG2 hepatoblastoma-derived cell line was purchased from LGC Standards (Cat# HB-8065, RRID:CVCL_0027) and maintained in MEM (Gibco Cat#31095) supplemented with 10%FBS. All cell lines were amplified upon arrival, tested for absence of mycoplasma (EZ-PCR mycoplasma test kit) aliquoted and stored in liquid nitrogen until use. All experiments were performed with mycoplasma-free cells. The human cell line HepG2 was authenticated by STR profiling within the last three years.

Animal models

All animal experiments were conducted according to institutional ethical norms and national laws, following approval from the Italian Ministry of Health (D. No. 30/2013).

The conditional knock-out RuvBL1$^{hep+/-}$ mice were created crossing RuvBL1$^{floxed/floxed}$ (RuvBL1$^{f/f}$) mice[8] with an Albumin-Cre$^{+/+}$ mice (strain#003574, B6.Cg-Tg(Alb-cre)21Mgn/J) acquired from Jackson Laboratories.

Crossing RuvBL1$^{f/f}$ with AlbCre$^{+/+}$ mice generates 100% RuvBL1hep$^{+/-}$ offspring. RuvBL1$^{f/f}$ mice were used as control group.

Carcinogenesis

Two-weeks old RuvBL1$^{f/f}$ and RuvBL1$^{hep+/-}$ male mice were injected intraperitoneally with a single dose of N-nitrosodiethylamine (DEN, Sigma-Aldrich) 5mg/kg. Mice were then sacrificed after 3, 6, 9 and 12 months, using 10-12 mice of each genotype, per time point. A separate group of mice not treated with DEN was used as external control (5 mice per genotype per time point).

qPCR

RNA was extracted from whole liver using the RNeasy Mini kit (Qiagen) and complementary DNA was synthesized using the High-Capacity cDNA Reverse Transcription kit (LifeTechnologies). Gene expression in RuvBL1$^{f/f}$ and RuvBL1$^{hep+/-}$ mice (3 months-old, n=5 per genotype) was quantified by qPCR using the ΔΔCt method and β-2microglobulin as reference gene (selected after comparison with GAPH and β-actin). Master mix was SYBR Select (Applied Biosystems), thermal cycler was ABI PRISM 7000 and analysis was run on Data Assist Software (Applied Biosystems). P-values were calculated from the ΔCt distributions using Student's t-test.

TCGA analysis

The TCGA database was accessed on 21.12.2017 through the cBioPortal for cancer genomics[9,10] to retrieve RuvBL1 mRNA expression data in the Liver Hepatocellular Carcinoma cohort (LIHC). RUVBL1 mRNA

expression data was available for 373 patients, that were assigned to the HI_RUVBL1 or LOW_RUVBL1 groups based on a Z-score of ± 2. Twenty-nine (8%) out of 371 fully sequenced patients had a RUVBL1 Z-score >2 and were assigned to the HI_RUVBL1 group. The mRNA expression data of genes significantly enriched in the two groups was used to run a Gene Ontology analysis with GlueGo (Cytoscape app) using KEGG_20.11.2017 ontology database. Survival and Disease-free survival analysis were run through the GEPIA[11] webserver (http://gepia.cancer-pku.cn/index.html), using the following cut-off values: High RUVBL1=60%, Low RUVBL1=40%.

Additional methods

The additional methods Sample Collection, Histological Stain, Histopathology, Immunofluorescence, Immunohistochemistry, DHE staining, Genotyping, Transmission Electron Microscopy, In vivo tests, Next-Generation Sequencing, Partial Hepatectomy can be found in the supplementary methods online.

Statistics.

Statistical calculation was performed using GraphPad Prism. The non-parametric Mann Whitney test was used to compare groups with n=5, while the Student's t-test was used for groups with n=10. Box and whiskers graphs show the minimum, the 25th percentile, the median, the 75th percentile, and the maximum values. In vitro data are representative of at least 3 independent experiments. The number of animals in each group is given in figure legends or methods section.

Data availability

The data that support the findings of this study are available from the corresponding author upon reasonable request. Transcriptomic data have been deposited in the European Nucleotide Archive (ENA) at EMBL-EBI under accession number PRJEB34908 (https://www.ebi.ac.uk/ena/data/view/ PRJEB34908).

RESULTS

1- Hepatocyte-conditional RuvBL1 haploinsufficient mouse model

RuvBL1$^{hep+/-}$ mice were obtained by crossing RuvBL1$^{f/f}$ mice[8] with Albumin-Cre mice[12]. RuvBL1$^{hep+/-}$ mice were viable, apparently healthy and fertile. The deletion of the RuvBL1 floxed allele was confirmed by PCR on genomic DNA extracted from the livers of RuvBL1$^{hep+/-}$ mice (Suppl. Fig.1 panel A). RuvBL1 haploinsufficiency resulted in approximatively a 45% reduction of RuvBL1 protein level in whole liver extract (Suppl. Fig.1 panel B). Through immunohistochemistry, we observed no detectable changes in the expression pattern of RuvBL1 between floxed and hemizygous mice (Suppl. Fig.1 panel C).

2- Haploinsufficiency of RuvBL1 hampers hepatocyte proliferation *in vivo*.

Since RuvBL1 is indispensable for cell survival[8], the livers of RuvBL1$^{hep+/-}$ mice were analyzed for phenotypic changes and signs of damage. We found no noticeable differences between RuvBL1$^{f/f}$ and RuvBL1$^{hep+/-}$ mice with respect to liver histology (Fig.1 A) and number of senescent (SA-β-galactosidase-positive) or apoptotic (caspase-3 positive) cells (Suppl. Fig. 2 A, B). Consistently, serum transaminases were not elevated in RuvBL1 haploinsufficient mice (Suppl. Fig.2 C, D). However, RuvBL1$^{hep+/-}$ mice showed a

significant reduction in the number of proliferating hepatocytes, determined by PCNA and phospho-histone-H3 immunohistochemistry (Fig.1 B, C). The expression level of HGF and TGFβ, the main mitotic and differentiation factors for hepatocytes, respectively, were also significantly reduced in RuvBL1$^{hep+/-}$ mice (Fig.1 D). These results suggested that RuvBL1 haploinsufficiency reduces the basal hepatocyte turnover, possibly due to an impaired replication potential of hepatocytes. To address this specific point RuvBL1$^{hep+/-}$ and RuvBL1$^{f/f}$ were subjected to 2/3 partial hepatectomy. Forty-eight hours after hepatectomy the number of BrdU positive hepatocytes was strikingly reduced in the RuvBL1$^{hep+/-}$ mice by approximately 8-fold (Fig.1 E). These results clearly show that loss of one RuvBL1 allele impairs hepatocyte proliferation, affecting both the basal hepatocyte turnover and liver regeneration after hepatectomy. *In vitro*, silencing RuvBL1 reduced the growth rate of the non-transformed hepatocytic cell line AML-12 as well as of HCC cells lines Hepa1-6 and HepG2 (Fig.1 F), in accordance with previous reports [4].

3- RuvBL1 haploinsufficiency delays DEN-induced cancer onset but promotes its long-term progression.

To evaluate the role of RuvBL1 in HCC oncogenesis, RuvBL1$^{f/f}$ and RuvBL1$^{hep+/-}$ mice were injected with DEN and sacrificed after 3, 6, 9 and 12 months. Three months after DEN injection, diffuse hydropic dysplasia, nuclear atypia, multi focal necrosis and inflammation were found in both genotypes. Small foci of cellular alterations were found in 4 out of 10 RuvBL1$^{f/f}$ and 3 out of 10 RuvBL1$^{hep+/-}$ mice (only one per mouse in each genotype), no evidence of macroscopic tumors was found in any of the mice (not shown). After 6 months, very small macroscopic lesions (1-2mm) were detectable only in 4 out of 12 (25%) RuvBL1$^{f/f}$ and 2 out of 12 (16%) RuvBL1$^{hep+/-}$ mice (Fig.2 A). At the microscopic level however, proliferative

pre-neoplastic foci were readily identified by H/E stain, RuvBL1 or PCNA immunohistochemistry (Fig.2 A). The large majority of pre-neoplastic foci were identified as basophilic foci of altered hepatocytes (FAH) (29 out of 31 lesions in RuvBL1$^{f/f}$ mice and 17 out of 22 lesions in RuvBL1$^{hep+/-}$ mice), with minor prevalence of eosinophil foci (1/31 in RuvBL1$^{f/f}$ and 1/22 in RuvBL1$^{hep+/-}$), mixed foci (1/31 in RuvBL1$^{f/f}$ and 1/22 in RuvBL1$^{hep+/-}$) and clear cell foci (3/22 in RuvBL1$^{hep+/-}$ mice only). By this time point, RuvBL1$^{hep+/-}$ mice had developed significantly fewer and seemingly smaller nodules than floxed mice (Fig.2 A). Interestingly, RuvBL1 was overexpressed in these lesions compared to the adjacent tissue regardless of the mice genotype (Fig.2 A). Resembling human HCC, DEN-induced liver lesions had a strong cytoplasmic staining for RuvBL1 compared to the surrounding parenchyma [4]. Despite the initial delay, 9 and 12 months following DEN injection the number of macroscopic tumors developed in RuvBL1$^{hep+/-}$ mice was similar to that in RuvBL1$^{f/f}$ ones. Moreover, HCC nodules were significantly larger in RuvBL1$^{hep+/-}$ mice than in floxed ones (Fig.2 B). These unexpected findings suggest that the appearance of DEN-induced liver tumors is delayed in RuvBL1$^{hep+/-}$ mice, but their progression is accelerated at longer time points. The histopathological analysis of neoplastic lesions revealed a higher prevalence of HCC in RuvBL1$^{hep+/-}$ mice respect to RuvBL1$^{f/f}$ mice (38.5% vs 22%) after 9 months of progression, while after 12 months the prevalence of liver adenomas (HCA) and HCC was similar between the two genotypes (Suppl. Table 1). Indeed, the accelerated tumor growth rate in RuvBL1$^{hep+/-}$ mice is also made evident by the higher PCNA labelling within the tumors of these mice (Fig.2 C) and by the sharp increase in liver weight at the latter time point (Fig.2 D). To exclude the unlikely possibility that tumors in RuvBL1$^{hep+/-}$ mice arose from cells that have escaped the Cre-recombination, we analyzed by PCR the DNA extracted from the masses and confirmed that such lesions retain RuvBL1 haploinsufficiency (Suppl. Fig.3). This finding suggests that

RuvBL1 overexpression in haploinsufficient mice could result from a hyper-activation of the remaining wild-type allele and strengthens the concept that RuvBL1 actively participates in cancer development. Thus, RuvBL1 haploinsufficiency delays the onset of DEN-induced liver cancer, most likely due to the reduced hepatocyte turnover in the hemizygous mice. However, contrary to our expectations, once tumor nodules are formed, they grow faster in RuvBL1$^{hep+/-}$ mice than in floxed mice.

4- RuvBL1 haploinsufficiency alters liver metabolism.

Given the abovementioned results, we hypothesized that RuvBL1$^{hep+/-}$ mice may had developed a metabolic microenvironment facilitating cancer cell growth. This hypothesis was supported by the differences in blood biochemical parameters of RuvBL1$^{f/f}$ and RuvBL1$^{hep+/-}$ mice, collected at sacrifice during the DEN time-course experiment. Indeed, throughout tumor progression, blood glucose and cholesterol concentrations were consistently higher in RuvBL1$^{hep+/-}$ than in floxed mice (Fig.3 A). Triglycerides were higher in RuvBL1$^{hep+/-}$ mice 3 and 12 months after DEN injection, (Fig.3 A). The trend toward higher glycemia, cholesterolemia and triglyceridemia in RuvBL1$^{hep+/-}$ mice was confirmed also in mice not treated with DEN (Suppl Fig.4). These data are indicative of remarkable metabolic alteration taking place in RuvBL1$^{hep+/-}$ mice. Since hyperglycemia is a well-recognized risk factor for cancer, including HCC[13,14], we focused on the regulation of glucose homeostasis in RuvBL1$^{hep+/-}$ mice. RuvBL1$^{hep+/-}$ mice had reduced glucose tolerance and insulin sensitivity, as shown by the Oral Glucose Tolerance Test (OGTT) and Insulin Tolerance Test (ITT), respectively (Fig.3 B). Interestingly, blood glucose concentration dropped similarly in floxed and haploinsufficient mice up to 60 minutes after insulin administration but recovered

significantly faster in RuvBL1$^{hep+/-}$ mice, suggesting an increased glucose output from the liver. Thus, mice were challenged by the Pyruvate Tolerance Test (PTT) to evaluate the hepatic gluconeogenesis, which was indeed found to be clearly higher in RuvBL1$^{hep+/-}$ than in RuvBL1$^{f/f}$ mice (Fig.3 B). Moreover, serum insulin concentration was elevated in RuvBL1$^{hep+/-}$ mice which also had a significantly higher body weight and visceral fat content than their floxed counterpart. (Fig.3 C-E). PAS stain and transmission electron microscopy (TEM) showed that liver glycogen content is strikingly reduced in the livers of RuvBL1$^{hep+/-}$ respect to floxed mice (Suppl. Fig.5 A, B). RuvBL1$^{hep+/-}$ mice also developed a mild microvesicular steatosis, as assessed by ORO staining and TEM (Suppl. Fig.5 C, D). Taken together, these results show that the loss of one allele of the RuvBL1 affects liver's glucose utilization *in vivo*, thus blunting insulin sensitivity, impairing the build-up of glycogen storages and resulting in an increased liver gluconeogenesis and hyperglycemia. To disentangle the overall effect of RuvBL1 haploinsufficiency on hepatocyte gene expression, we performed liver whole-transcriptome analysis by NGS. Differentially expressed genes (DEGs) were identified using either DESeq2 or EdgeR software, yielding 242 and 251 DEGs, respectively, of which 176 (about 70% of the genes in each list) were identified by both software packages (Suppl. Table 2). Gene Ontology analysis performed using the common genes set confirmed that a large portion of the significantly modulated biological processes is related to glucose metabolism and homeostasis, as well as lipid and cholesterol metabolism (Fig.4). Taken together, these results clearly demonstrate that hepatic RuvBL1 is a major regulator of whole-body metabolism, strongly impacting liver glucose homeostasis and insulin sensitivity. We next moved to investigate the molecular mechanisms underlying this metabolic phenotype and its implications to HCC development.

5- RuvBL1 is required for effective Akt-mTOR signaling *in vitro* and *in vivo*.

The effect of RuvBL1 silencing on insulin signaling was investigated *in vitro* in the non-transformed hepatocytic cell line AML-12. Insulin induced the phosphorylation of Akt(Ser473), mTOR(Ser2448) and of their down-stream effectors FOXO3A and S6 in AML-12 cells silenced with the negative-control siRNA. In RuvBL1-silenced cells, both basal and insulin-induced phosphorylation of AKT, mTOR, FOXO3A and S6 were clearly blunted (Fig.5 A). To recapitulate these findings *in vivo*, RuvBL1$^{hep+/-}$ and floxed mice were fasted for 6 hours and then either re-fed ad libitum for 1 hour or i.p. injected with insulin 0.1U/Kg. Following refeeding or insulin administration, phosphorylation levels of Akt(Ser473), mTOR, and GSK3α/β(Ser9/21) were markedly reduced in RuvBL1$^{hep+/-}$ mice compared to floxed mice (Fig.5 B). Moreover, nuclear exclusion of FOXO1 following insulin administration, which occurs after its phosphorylation downstream the insulin signaling pathway, was impaired in the livers of fasted RuvBL1$^{hep+/-}$ mice, but not in those of fasted RuvBL1$^{f/f}$ mice (Fig.5 C). Clearly, downregulation of RuvBL1 affects insulin signaling both *in vitro* and *in vivo*. RuvBL1 has been shown to regulate the abundance of PIKKs family members, including mTOR[15,16], and RuvBL1 containing complexes, such as R2TP/Prefoldin-like and TTT-RVB1/2, play a major role in mTORC1 intracellular localization and activation[17,18]. Consistently, silencing RuvBL1 reduced basal mTOR expression and phosphorylation in all three cell lines tested, AML-12, Hepa1-6 and HepG2 (Fig.5 A, D). Moreover, direct mTORC1 transcriptional targets such as PPARɣ, SREBP1c, together with downstream PPARɣ targets such as LXRα and LXRβ, were downregulated at mRNA level in RuvBL1$^{hep+/-}$ mice, further substantiating that the mTOR signaling pathway is disrupted in RuvBL1hep$^{+/-}$ mice (Fig.5 E). As we observed by immunohistochemistry that RuvBL1 was similarly overexpressed in DEN-induced nodules of RuvBL1$^{hep+/-}$ and floxed mice (Fig.2 A), we

investigated mTOR expression in this context. Paralleling RuvBL1 expression, mTOR was found reduced in the non-tumor areas of RuvBL1$^{hep+/-}$ mice, but up-regulated in DEN-induced HCC of both floxed and hemizygous mice (Fig.5 F). Taken together, these results clearly demonstrate that targeting RuvBL1 strongly affects mTOR expression level and insulin signaling through the Akt/mTOR pathway *in vivo* and in normal AML-12 liver cells. Moreover, mTOR parallels RuvBL1 expression levels in DEN-induced tumors and HCC cell lines.

6- RuvBL1 expression correlates with glucose metabolic gene expression and reduced survival in human HCC.

Based on our experimental results, we speculated that HCC cells may exploit RuvBL1 overexpression to boost the activity of the Akt/mTOR pathway whereby driving a metabolic switch towards increased glucose utilization and anabolic metabolism. To explore this scenario in human HCC, we took advantage of the The Cancer Genome Atlas (TCGA) database. The TCGA was accessed using cBioPortal to retrieve the set of genes with the highest expression correlation to RUVBL1 in the liver hepatic cancer cohort of patients (LIHC). We identified 29 out of 371 (8%) HCC samples in which RuvBL1 expression was at least twice the average expression in the LIHC cohort (Z-score > +2). The expression of 560 genes significantly correlated with RuvBL1 (Suppl. Table 3) in the LIHC cohort (q-value <0.05) and were used to run a Gene Set Enrichment Analysis (GSEA) and Gene Ontology (GO) analysis. We found that glucose metabolism was a significantly enriched GO term in RuvBL1-coexpressed genes, together with several biological functions that are already known to be regulated by RuvBL1, such as RNA processing, ribosome biogenesis, DNA

replication and cell cycle progression[2,19] (Fig.6 A). GSEA further identified several hallmarks gene sets as positively correlated with high RuvBL1-expressing HCC: E2F targets, G2M checkpoint, MYC-targets and mTORC1 signalling (Fig.6 B). Finally, HCC patients with high RUVBL1 expression showed a significantly reduced overall survival and disease-free survival (Fig.6 C, D).

DISCUSSION

RuvBL1 is overexpressed in several human cancers[3] and it expression correlate with poor prognosis in HCC patients[4]. Targeting RuvBL1 effectively reduces HCC cell growth in vitro[4,5], nevertheless, whether and how RuvBL1 contributes to HCC development is still unknown. In this work, we expressly created a RuvBL1 hepatocyte-conditional haploinsufficient mouse model and tested whether targeting RuvBL1 could reduce DEN-induced HCC onset and progression. We found that in these mice the reduced RuvBL1 expression was *per se* sufficient to impair the basal hepatocyte turnover (Fig.1 B, C) and liver regenerative potential after 2/3 hepatectomy (Fig.1 E), consistently with the evolutionarily conserved role of RuvBL1 in cell growth and mitosis[20]. Six months after DEN administration, RuvBL1$^{hep+/-}$mice developed fewer and smaller nodules than floxed mice (Fig.2 A). Of importance, RuvBL1 expression was found downregulated in the normal parenchyma of RuvBL1$^{hep+/-}$ mice but not within the DEN-induced altered hepatocyte foci, which suggests that overexpression of this gene is indeed required for tumor development (Fig.2 A). The mid-term reduction in carcinogenesis in RuvBL1$^{hep+/-}$ mice can be reasonably ascribed to the reduced hepatocyte turnover in these mice, which allegedly slows down the promoting phase of DEN cancerogenesis. Since the expression of several Cyp was found downregulated by whole transcriptome

analysis in haploinsufficient mice (Suppl. Table 2), we cannot completely rule out that the metabolic activation of DEN by the P450 system may had been reduced, whereby decreasing its carcinogenicity in these animals. The potential impact of litter differences on DEN initiation should also be considered as a possible confounding factor. However, by long-term tumor progression (9 and 12 months) RuvBL1$^{hep+/-}$ and floxed mice had developed approximatively the same number of macroscopic tumors (Fig.2 B), arguing against any significant difference in the initial oncogenic DEN hit between the two mouse strains. Indeed, CYP2E1, which plays a major role in DEN activation in mice[21], was not among the P450 isoforms affected in RuvBL1$^{hep+/-}$ mice (Suppl. Table 2). Unexpectedly, at the later time points RuvBL1$^{hep+/-}$ mice developed significantly larger tumors that control mice (Fig.2 B). Moreover, the histopathological analysis showed that after 9 months of progression the prevalence of HCC in RuvBL1$^{hep+/-}$ mice was almost twice as much than in floxed mice, while at 12 months a similar prevalence of HCA and HCC was found in the two genotypes (Suppl. Table 1). Therefore, despite the initial delay, tumors arose in RuvBL1$^{hep+/-}$ mice were able to grow and progress faster, as confirmed by the higher PCNA labelling index (Fig.2, C). This bi-phasic effect suggests a divergent role of RuvBL1 on DEN-induced tumor initiation and progression. However, to disentangle the relative contribution of RuvBL1 to these two processes would require a combination of Cre-inducible models and different DEN protocols, which goes beyond the scope of this manuscript. Based on blood biochemical parameters (Fig.3 A), we hypothesized that a permissive microenvironment could promote HCC growth in RuvBL1$^{hep+/-}$ mice. In fact, we found that RuvBL1 haploinsufficiency *per se* strongly alters the hepatic glucose metabolism, leading to hyperglycemia, increased hepatic gluconeogenesis, hyper-insulinemia and hepatic insulin resistance (Fig.3 B-C and suppl. Fig.4). Moreover, RuvBL1$^{hep+/-}$ mice had higher body weight and visceral FAT content (Fig. 3 D, E) therefore displaying a metabolic phenotype

in line of what is defined as "metabolic syndrome" (MS). Obesity, diabetes, hyperglycemia and MS are well known risk factors for cancer including HCC[13,14]. It is therefore conceivable that the haploinsufficiency of RuvBL1 on one hand hampers the hepatocyte proliferation potential therefore delaying tumor onset, but on the other hand deranges liver glucose metabolism towards a cancer-promoting environment. Supporting this line of thoughts, whole transcriptomic profiling via NGS confirmed that the largest proportion of affected biological functions in RuvBL1$^{hep+/-}$ mice are related to glucose metabolic process, including the insulin receptor signaling pathway (Fig.4). From a mechanistic perspective, insulin signals through the insulin receptor to the PI3K/Akt/mTOR pathway, which branches the signaling pathway out to several downstream effectors. Insulin-induced activation of Akt requires phosphorylation on Ser473, which is mediated by the mTORC2 complex[22,23]. Accumulating *in vitro* evidences link RuvBL1-containing complexes to the mTOR pathway at multiple levels. In fact, several RuvBL1-containig complexes interacts with and regulates the abundance of mTOR[15,16,24] as well as mTORC1 localization and activity[17,18]. Nonetheless, direct *in vivo* evidence of RuvBL1 action on the PI3K/Akt/mTOR pathway was still missing. We have shown here that RuvBL1$^{hep+/-}$ mice had reduced mTOR protein levels (Fig.5 B, F), impaired insulin-induced Akt phosphorylation and reduced mTORC1/2 signaling (Fig.5 B, C). Since a downregulation of mTOR protein levels could in principle affect both mTORC1 and mTORC2 complexes, the impaired Akt phosphorylation after stimulation by insulin in RuvBL1$^{hep+/-}$ mice and RuvBL1-silenced cells (Fig.5 A, B) could well mirror a reduction of mTORC2 activity. Indeed, RuvBL1$^{hep+/-}$ mice are remarkably similar to Rictor LI-KO mice with respect to glucose metabolism[25]. In fact, RuvBL1$^{hep+/-}$ mice have reduced liver glycogen content (Suppl. Fig.5 A, B) hepatic insulin resistance and constitutive hepatic gluconeogenesis (Fig.3 B), hyperglycemia (Fig.3 A and Suppl. Fig.4) and hyperinsulinemia (Fig.3 C), all of which are common

features of Rictor LI-KO mice. Moreover, we showed that insulin/feeding signaling is also affected downstream PI3K/Akt/mTORC1 in RuvBL1$^{hep+/-}$ and in RuvBL1-silenced AML-12 cells. Consistently, mTORC1 transcriptional targets such as SREBF1 and PPARɣ are downregulated in ad-libitum fed RuvBL1$^{hep+/-}$ mice (Fig.5 E). Interestingly, LXR-α and -β, which are well known to mediate insulin-dependent induction of Srebp-1c mRNA[26,27] are also downregulated in RuvBL1 haploinsufficient mice (Fig.5 E). Indeed, LXRs have been proposed as the mediators of mTORC1-dependent induction of SREBP mRNA[28] and although the molecular mechanism are still to be elucidated, recent observations in macrophages support this line of thoughts[29]. Moreover, LXRα is a known transcriptional target of PPARɣ[30,31], which in turn is a *bona fide* mTORC1 target[32]. Therefore, LXRs downregulation in RuvBL1$^{hep+/-}$ mice could be interpreted in the light of the reduced activity of mTORC1. Inhibition of mTORC1 signaling activates the ketogenic response in mice by upregulation of PPARα and β-oxidation[33,34]. Consistently with a reduced activity of mTORC1 complex, RuvBL1$^{hep+/-}$ mice showed an upregulation of PPARα, of its target gene CD36 and an increased production of mitochondrial-related ROS (Suppl. Fig.6 A, B). Interestingly, downregulation of PPARɣ and SREBF1, as well as upregulation of PPARα and CD36 are also observed in Rictor LI-KO mice[25]. However, mTORC2 inhibition alone results in reduced plasma cholesterol and triglycerides, as well as reduced liver lipid content, opposite of what we found in RuvBL1$^{hep+/-}$ mice (Fig.3 A, Suppl. Fig.4 and Suppl. Fig.5). During the drafting of this manuscript, we became aware of a report on opposite mTORC1 and mTORC2 regulation by hepatic RuvBL2/Reptin[35]. Despite the fact that depletion of RuvBL2 affects mTOR protein levels, similarly to what we observe with RuvBL1, Reptin^{LIKO} mice showed an improved glucose metabolism and reduced gluconeogenesis on chow and HFD diet. Loss of mTOR expression in these mice affected mTORC1 function while enhancing mTORC2 activity. Therefore, RuvBL1 and RuvBL2 seems to

play opposite roles on liver glucose metabolism, most likely through a divergent action on the mTORC2 complex activity, the mechanistic basis of which is still undetermined. As the mTOR pathway is deregulated in up to 50% of HCC[36] it is tempting to speculate that HCC cells can exploit RuvBL1 overexpression to support an mTOR-driven metabolic rewiring to promote cell growth. Consistently, RuvBL1 silencing in mice and human HCC cells reduces their growth potential (Fig.1 F), which is paralleled by a downregulation of mTOR expression (Fig.5 D). Moreover, RuvBL1 and mTOR expression is reduced in the non-tumoral parenchyma of RuvBL1$^{hep+/-}$ mice but overexpressed in DEN-induced tumors (Fig.5 F), suggesting a positive correlation between RuvBL1 expression and the mTOR pathway in HCC. We therefore consulted the TCGA database to explore this hypothesis in human HCC samples. The set of genes whose expression correlates with RuvBL1 in human HCC turned out to be significantly enriched in Hallmark Genes for the E2F targets, MYC targets, G2M Checkpoint (all known functions of RuvBL1) and mTORC1 pathway (Fig.6 B and Suppl. Table 4). Moreover, KEGG pathway analysis shows that glucose metabolism is a significant enriched function associated with RuvBL1 expression in human HCC (Fig.6 A). Thus, RuvBL1 overexpression seems to promote the mTOR pathway activity and metabolic rewiring in human HCC, providing a mechanistic insight for its overexpression in cancer cells.

In conclusion, we reported here for the first time the effect of liver-specific RuvBL1 knock-down on hepatic carcinogenesis. Our data uncovered the key role of RuvBL1 at the intersection of liver metabolism, hepatocyte proliferation and HCC development. As RuvBL1 is emerging as a potential molecular target in several human cancers[37], our results prompt to a cautionary approach towards inhibition of this ATPase, if not selectively restricted to cancer cells. In the light of these results, it will be crucial to further clarify the physiologic versus pro-tumoral metabolic functions of RuvBL1 in future studies.

Acknowledgements

We are grateful to Dr. Marco Bruttini at Polo GGB (Siena, Italy) for continued support in the bioinformatics analysis of NGS data.

Financial support

This research was supported by the Italian Ministry of Health through grant GR-2009-1600315 and by Ente CRF Firenze through Grant 2013.0673.

Conflict of Interests

The authors declare no competing interests

Author contribution: § these authors contributed equally.

Conceptualization, T.M.; Methodology, T.M., M.M., F.Z.; Investigation; T.M., M.M., F.Z., I.S., E.C., S.P., M.T., G.M., D.G., D.B.; Writing – Original Draft, T.M.; Writing – Review & Editing, T.M., M.M. O.B. M.P. I.S. and A.G.; Funding Acquisition, T.M.; Resources, O.B., C.N., D.G., D.B.; Supervision, T.M. and A.G.

References

1. Ferlay J, Soerjomataram I, Dikshit R, Eser S, Mathers C, Rebelo M, Parkin DM, Forman D, Bray F. Cancer incidence and mortality worldwide: sources, methods and major patterns in GLOBOCAN 2012. *Int J Cancer* 2015;136:E359-E386.

2. Mao YQ, Houry WA. The Role of Pontin and Reptin in Cellular Physiology and Cancer Etiology. *Front Mol Biosci* 2017;4:58.

3. Grigoletto A, Lestienne P, Rosenbaum J. The multifaceted proteins Reptin and Pontin as major players in cancer. *Biochim Biophys Acta* 2011;1815:147-57.

4. Haurie V, Menard L, Nicou A, Touriol C, Metzler P, Fernandez J, Taras D, Lestienne P, Balabaud C, Bioulac-Sage P, Prats H, Zucman-Rossi J, et al. Adenosine triphosphatase pontin is overexpressed in hepatocellular carcinoma and coregulated with reptin through a new posttranslational mechanism. *Hepatology* 2009;50:1871-83.

5. Elkaim J, Castroviejo M, Bennani D, Taouji S, Allain N, Laguerre M, Rosenbaum J, Dessolin J, Lestienne P. First identification of small-molecule inhibitors of Pontin by combining virtual screening and enzymatic assay. *Biochem J* 2012;443:549-59.

6. Breig O, Bras S, Martinez SN, Osman D, Heidenreich O, Haenlin M, Waltzer L. Pontin is a critical regulator for AML1-ETO-induced leukemia. *Leukemia* 2014;28:1271-9.

7. Yuan XS, Wang ZT, Hu YJ, Bao FC, Yuan P, Zhang C, Cao JL, Lv W, Hu J. Downregulation of RUVBL1 inhibits proliferation of lung adenocarcinoma cells by G1/S phase cell cycle arrest via multiple mechanisms. *Tumour Biol* 2016.

8. Bereshchenko O, Mancini E, Luciani L, Gambardella A, Riccardi C, Nerlov C. Pontin is essential for murine hematopoietic stem cell survival. *Haematologica* 2012;97:1291-4.

9. Gao J, Aksoy BA, Dogrusoz U, Dresdner G, Gross B, Sumer SO, Sun Y, Jacobsen A, Sinha R, Larsson E, Cerami E, Sander C, et al. Integrative analysis of complex cancer genomics and clinical profiles using the cBioPortal. *Sci Signal* 2013;6:l1.

10. Cerami E, Gao J, Dogrusoz U, Gross BE, Sumer SO, Aksoy BA, Jacobsen A, Byrne CJ, Heuer ML, Larsson E, Antipin Y, Reva B, et al. The cBio cancer genomics portal: an open platform for exploring multidimensional cancer genomics data. *Cancer Discov* 2012;2:401-4.

11. Tang Z, Li C, Kang B, Gao G, Li C, Zhang Z. GEPIA: a web server for cancer and normal gene expression profiling and interactive analyses. *Nucleic Acids Res* 2017;45:W98-W102.

12. Postic C, Shiota M, Niswender KD, Jetton TL, Chen Y, Moates JM, Shelton KD, Lindner J, Cherrington AD, Magnuson MA. Dual roles for glucokinase in glucose homeostasis as determined by liver and pancreatic beta cell-specific gene knock-outs using Cre recombinase. *J Biol Chem* 1999;274:305-15.

13. Younossi ZM, Koenig AB, Abdelatif D, Fazel Y, Henry L, Wymer M. Global epidemiology of nonalcoholic fatty liver disease-Meta-analytic assessment of prevalence, incidence, and outcomes. *Hepatology* 2016;64:73-84.

14. El-Serag HB, Rudolph KL. Hepatocellular carcinoma: epidemiology and molecular carcinogenesis. *Gastroenterology* 2007;132:2557-76.

15. Izumi N, Yamashita A, Iwamatsu A, Kurata R, Nakamura H, Saari B, Hirano H, Anderson P, Ohno S. AAA+ proteins RUVBL1 and RUVBL2 coordinate PIKK activity and function in nonsense-mediated mRNA decay. *Sci Signal* 2010;3:ra27.

16. Horejsi Z, Takai H, Adelman CA, Collis SJ, Flynn H, Maslen S, Skehel JM, de LT, Boulton SJ. CK2 phospho-dependent binding of R2TP complex to TEL2 is essential for mTOR and SMG1 stability. *Mol Cell* 2010;39:839-50.

17. Kim SG, Hoffman GR, Poulogiannis G, Buel GR, Jang YJ, Lee KW, Kim BY, Erikson RL, Cantley LC, Choo AY, Blenis J. Metabolic stress controls mTORC1 lysosomal localization and dimerization by regulating the TTT-RUVBL1/2 complex. *Mol Cell* 2013;49:172-85.

18. Cloutier P, Poitras C, Durand M, Hekmat O, Fiola-Masson E, Bouchard A, Faubert D, Chabot B, Coulombe B. R2TP/Prefoldin-like component RUVBL1/RUVBL2 directly interacts with ZNHIT2 to regulate assembly of U5 small nuclear ribonucleoprotein. *Nat Commun* 2017;8:15615.

19. Jha S, Dutta A. RVB1/RVB2: running rings around molecular biology. *Mol Cell* 2009;34:521-33.

20. Ducat D, Kawaguchi S, Liu H, Yates JR, III, Zheng Y. Regulation of microtubule assembly and organization in mitosis by the AAA+ ATPase Pontin. *Mol Biol Cell* 2008;19:3097-110.

21. Kang JS, Wanibuchi H, Morimura K, Gonzalez FJ, Fukushima S. Role of CYP2E1 in diethylnitrosamine-induced hepatocarcinogenesis in vivo. *Cancer Res* 2007;67:11141-6.

22. Hresko RC, Mueckler M. mTOR.RICTOR is the Ser473 kinase for Akt/protein kinase B in 3T3-L1 adipocytes. *J Biol Chem* 2005;280:40406-16.

23. Guertin DA, Stevens DM, Thoreen CC, Burds AA, Kalaany NY, Moffat J, Brown M, Fitzgerald KJ, Sabatini DM. Ablation in mice of the mTORC components raptor, rictor, or mLST8 reveals that mTORC2 is required for signaling to Akt-FOXO and PKCalpha, but not S6K1. *Dev Cell* 2006;11:859-71.

24. Izumi N, Yamashita A, Hirano H, Ohno S. Heat shock protein 90 regulates phosphatidylinositol 3-kinase-related protein kinase family proteins together with the RUVBL1/2 and Tel2-containing co-factor complex. *Cancer Sci* 2012;103:50-7.

25. Hagiwara A, Cornu M, Cybulski N, Polak P, Betz C, Trapani F, Terracciano L, Heim MH, Ruegg MA, Hall MN. Hepatic mTORC2 activates glycolysis and lipogenesis through Akt, glucokinase, and SREBP1c. *Cell Metab* 2012;15:725-38.

26. Chen G, Liang G, Ou J, Goldstein JL, Brown MS. Central role for liver X receptor in insulin-mediated activation of Srebp-1c transcription and stimulation of fatty acid synthesis in liver. *Proc Natl Acad Sci U S A* 2004;101:11245-50.

27. Sun X, Haas ME, Miao J, Mehta A, Graham MJ, Crooke RM, Pais de Barros JP, Wang JG, Aikawa M, Masson D, Biddinger SB. Insulin Dissociates the Effects of Liver X Receptor on Lipogenesis, Endoplasmic Reticulum Stress, and Inflammation. *J Biol Chem* 2016;291:1115-22.

28. Laplante M, Sabatini DM. mTORC1 activates SREBP-1c and uncouples lipogenesis from gluconeogenesis. *Proc Natl Acad Sci U S A* 2010;107:3281-2.

29. Kimura T, Nada S, Takegahara N, Okuno T, Nojima S, Kang S, Ito D, Morimoto K, Hosokawa T, Hayama Y, Mitsui Y, Sakurai N, et al. Polarization of M2 macrophages requires Lamtor1 that integrates cytokine and amino-acid signals. *Nat Commun* 2016;7:13130.

30. Juvet LK, Andresen SM, Schuster GU, Dalen KT, Tobin KA, Hollung K, Haugen F, Jacinto S, Ulven SM, Bamberg K, Gustafsson JA, Nebb HI. On the role of liver X receptors in lipid accumulation in adipocytes. *Mol Endocrinol* 2003;17:172-82.

31. Laffitte BA, Joseph SB, Walczak R, Pei L, Wilpitz DC, Collins JL, Tontonoz P. Autoregulation of the human liver X receptor alpha promoter. *Mol Cell Biol* 2001;21:7558-68.

32. Laplante M, Sabatini DM. mTOR signaling at a glance. *J Cell Sci* 2009;122:3589-94.

33. Kim K, Pyo S, Um SH. S6 kinase 2 deficiency enhances ketone body production and increases peroxisome proliferator-activated receptor alpha activity in the liver. *Hepatology* 2012;55:1727-37.

34. Sengupta S, Peterson TR, Laplante M, Oh S, Sabatini DM. mTORC1 controls fasting-induced ketogenesis and its modulation by ageing. *Nature* 2010;468:1100-4.

35. Javary J, Allain-Court, Saucisse N, Costet P, Heraud C, Benhamed F, Pierre R, Bure C, Pallares-Lupon N, Do CM, Postic C, Cota D, et al. Liver Reptin/RUVBL2 controls glucose and lipid metabolism with opposite actions on mTORC1 and mTORC2 signalling. *Gut* 2017.

36. Villanueva A, Chiang DY, Newell P, Peix J, Thung S, Alsinet C, Tovar V, Roayaie S, Minguez B, Sole M, Battiston C, Van LS, et al. Pivotal role of mTOR signaling in hepatocellular carcinoma. *Gastroenterology* 2008;135:1972-83, 1983.

37. Assimon VA, Tang Y, Vargas JD, Lee GJ, Wu ZY, Lou K, Yao B, Menon MK, Pios A, Perez KC, Madriaga A, Buchowiecki PK, et al. CB-6644 Is a Selective Inhibitor of the RUVBL1/2 Complex with Anticancer Activity. *ACS Chem Biol* 2019;14:236-44.

FIGURE LEGENDS

Fig.1 Haploinsufficiency of RuvBL1 hampers hepatocyte proliferation. **A)** Eosin/Hematoxylin of liver sections. Scale bar = 100um **B)** PCNA immunofluorescence of 3months-old mice and quantitation (n=5 per genotype, mean ± SD) Scale bar = 100um **C)** phospho-histone H3 immunofluorescence of 3months-old mice and quantitation (n=5 per genotype, mean ± SD). Scale bar = 50um **D)** Relative RNA expression in liver of 3 months-old mice (n=5 per genotype) **E)** BrdU immunofluorescence of liver sections 48 hours after 2/3 hepatectomy (n=5 per genotype, mean ± SD). Scale bar = 100um **F)** Growth curve of cell lines silenced with RuvBL1 siRNA or Control siRNA (n=3, mean ± SD). *p<0.05, **p<0.01

Fig.2 DEN-induced liver carcinogenesis. A) 6 months after DEN injection small macroscopic lesions are visible only in RuvBL1f/f mice. Microscopic lesions are apparent by H/E staining, RuvBL1 overexpression and PCNA positivity in both genotypes. Scale bar=100um. Graphs show tumors number and size in mice 6 months after DEN injection. Data presented as mean ± SEM (n=12 per genotype). B) Livers of $RuvBL1^{f/f}$ and $RuvBL1^{hep+/-}$ mice 12 months after DEN induction. Tumor number and size (maximal length in mm) of macroscopic tumors 9 and 12 months after DEN injection (n=10 per genotype) are shown in graphs. C) PCNA immunohistochemistry and PCNA labelling index in mice 9 months after DEN injection (mean ± SEM). D) Liver weight (normalized to body weight) during cancer progression (mean ± SEM; n=10 per genotype). *p<0.05, **p<0.01.

Fig.3 RuvBL1 haploinsufficiency alters liver metabolism. A) Serum glucose, triglycerides and cholesterol concentrations measured at sacrifice in DEN-treated RuvBL1$^{f/f}$ and RuvBL1$^{hep+/-}$ mice (mean ± SEM ; n=10 per genotype per time point). See Suppl. Fig. 4 for serum glucose, triglycerides and cholesterol concentrations of mice not treated with DEN. B) Oral Glucose Tolerance Test, Insulin Tolerance Test, Pyruvate Tolerance Test (n=5 per genotype, 3 months old mice). C) Insulin serum concentration in 3 months old mice (n=5 per genotype) D) Visceral fat content (n=5 per genotype per time point) E) Body weight (n=5 per genotype per time point). *p<0.05, **p<0.01, ***p<0.001, ****p<0.0001

Fig.4 Liver whole transcriptome analysis by NGS. Gene Ontology analysis of differentially expressed genes (DEG) in livers of 3 months-old RuvBL1$^{f/f}$ and RuvBL1$^{hep+/-}$ mice. Pie chart shows the relative abundance of GO categories in differentially expressed genes. The number of DEG annotated in each GO term and their relative coverage of the GO term are displayed in the bar chart. (also see Supp. Table 2 for a list of DEG in RuvBL1$^{f/f}$ and RuvBL1$^{hep+/-}$)

Fig.5 RuvBL1 is required for effective Akt-mTOR signaling *in vitro* and *in vivo.* A) Insulin signaling is reduced in RuvBL1-silenced AML12 cells B) Insulin signaling is reduced in fasted-refed or fasted+insulin RuvBL1$^{hep+/-}$ mice C) Immunofluorescence showing hepatic FOXO1A localization after insulin administration to RuvBL1$^{f/f}$ and RuvBL1$^{hep+/-}$ mice. Scale bar=100um. D) mTOR and phospho-mTOR levels in RuvBL1-silenced hepatic cell lines. E) mRNA expression of transcriptional mTOR targets in livers of 3 months-old RuvBL1$^{f/f}$ and RuvBL1$^{hep+/-}$ mice (n=5 per genotype). F) RuvBL1 and mTOR protein expression

within the normal parenchyma and HCC in RuvBL1$^{f/f}$ and RuvBL1$^{hep+/-}$ mice. Relative expression reported as mean ± SEM

Fig.6 High RuvBL1 expression is associated with glucose metabolism, mTORC1 hallmark and reduced survival in human HCC patients. A) Gene ontology analysis (KEGG) of genes significantly enriched in high- vs low- RuvBL1-expressing HCC samples in the TCGA LIHC cohort. See Suppl. Table 3 for the full list of enriched genes. B) GSEA analysis on the same dataset showing significantly-enriched Hallmarks (FDR<0.05). See Suppl. Table 4 for GSEA statistics C-D) Survival and Disease-free survival in high- vs low-RuvBL1 expressing HCC patients in the TCGA-LIHC cohort.

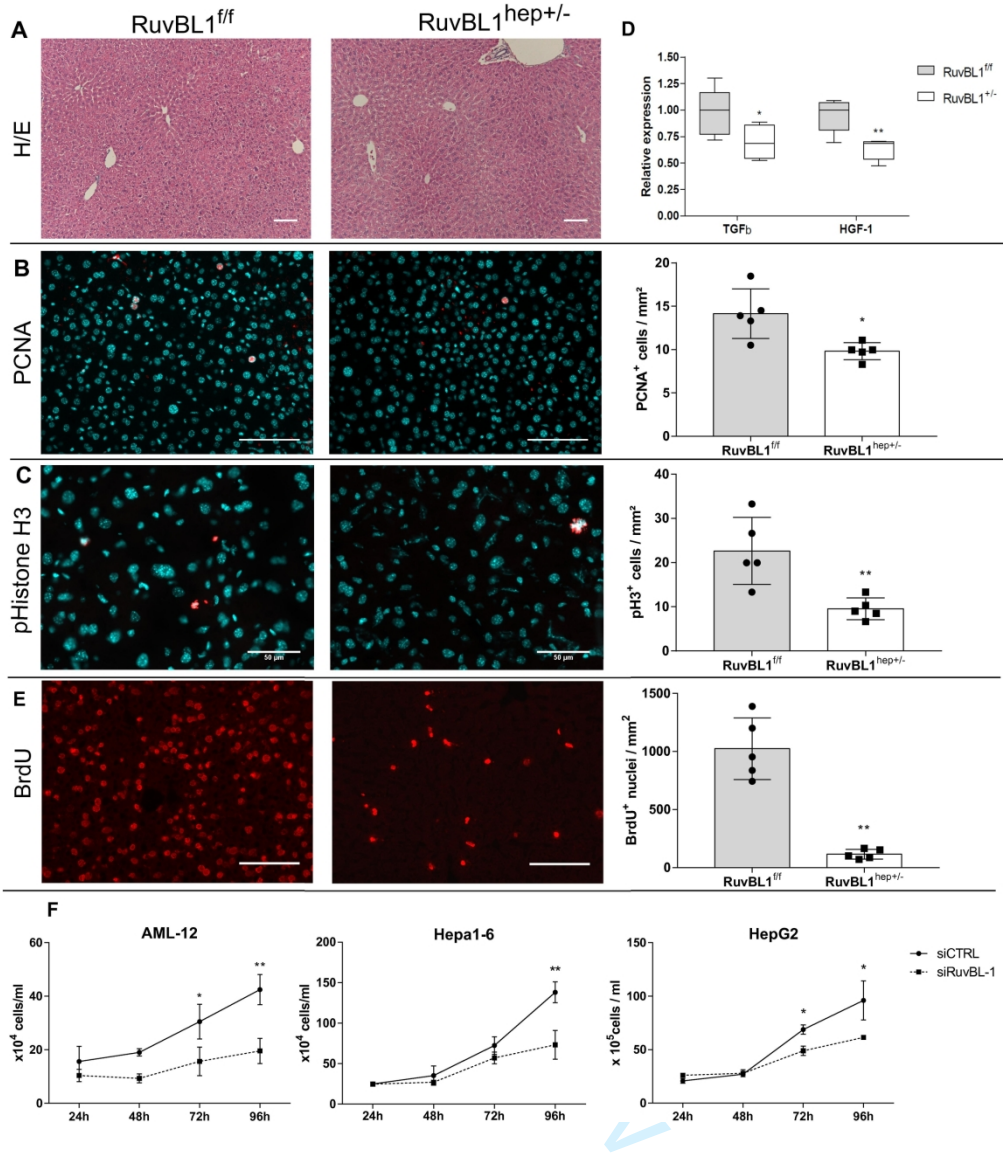

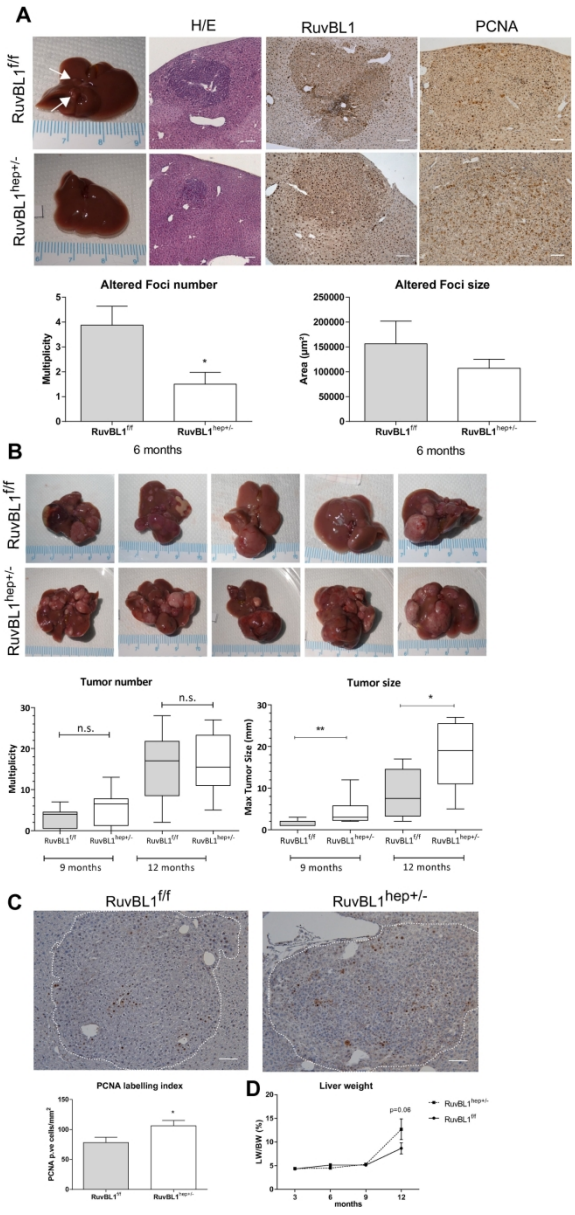

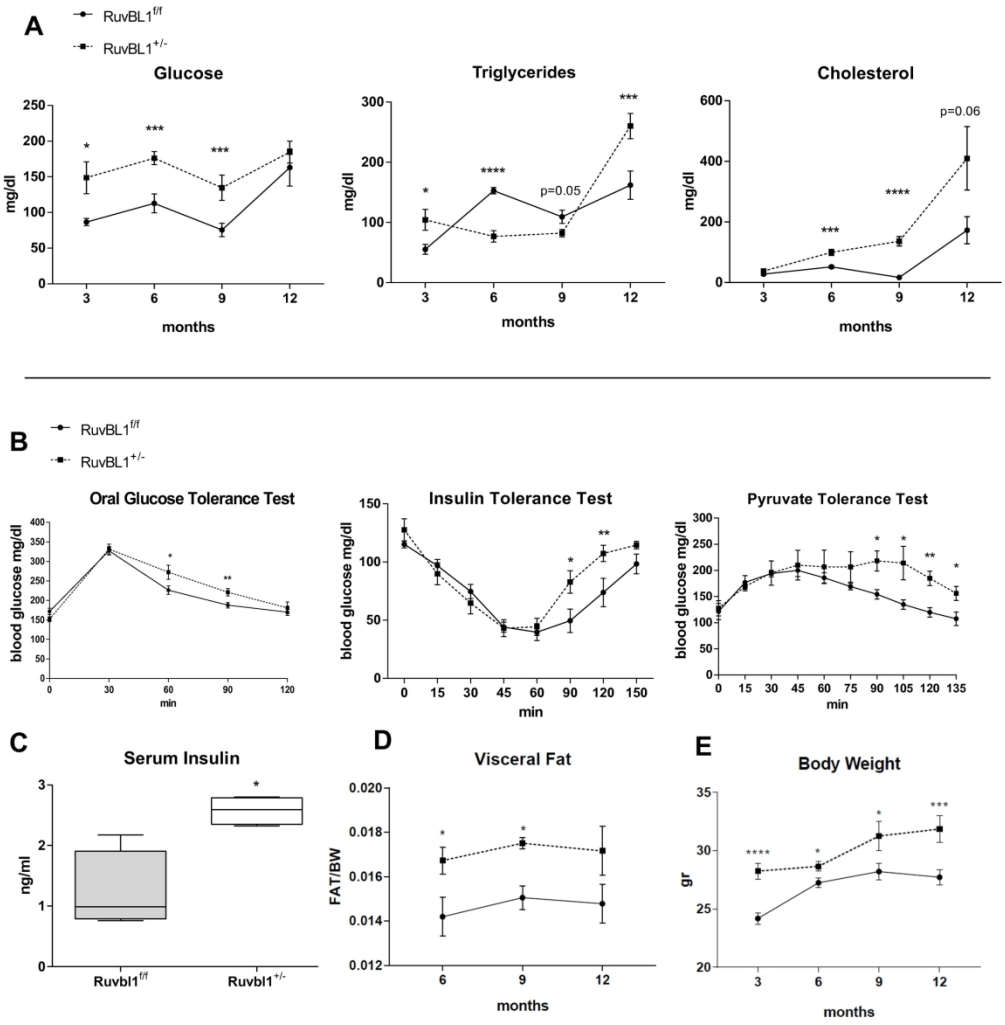

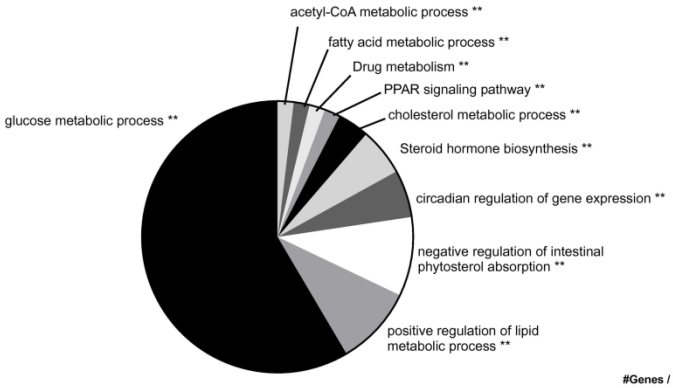

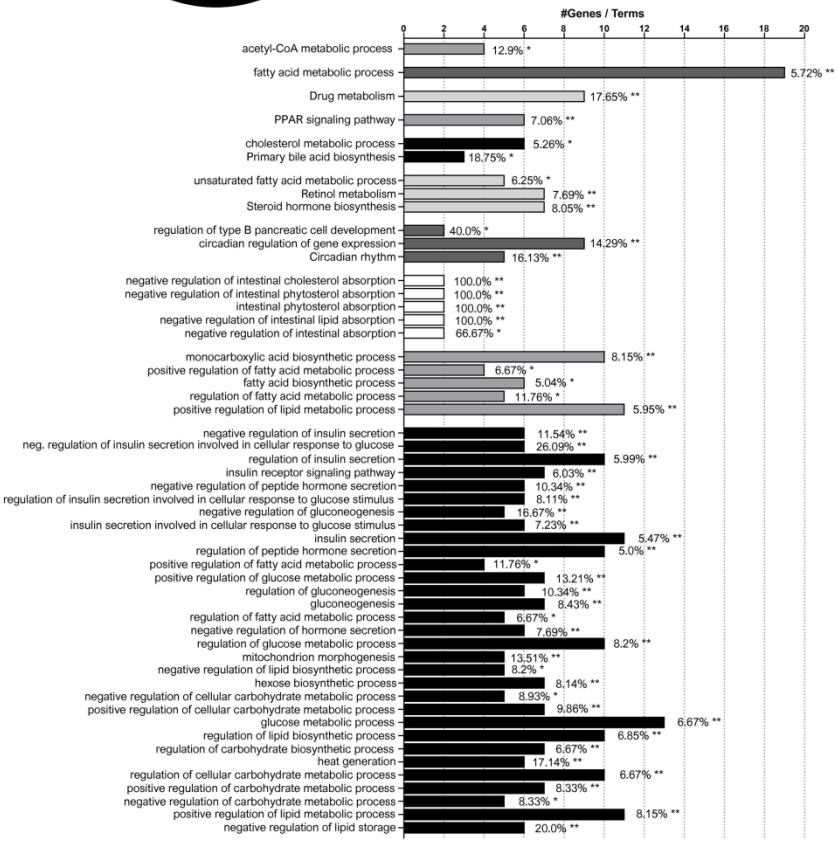

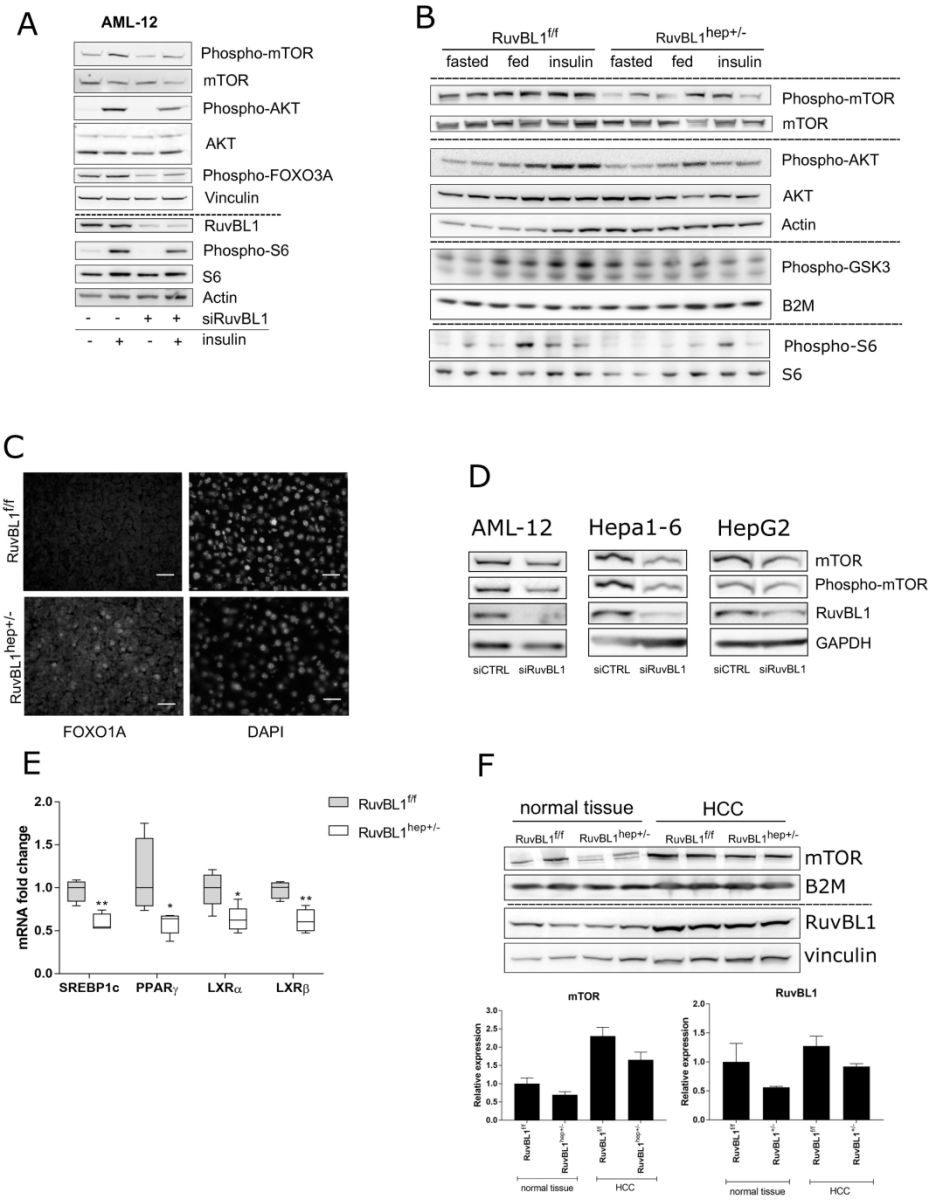

A

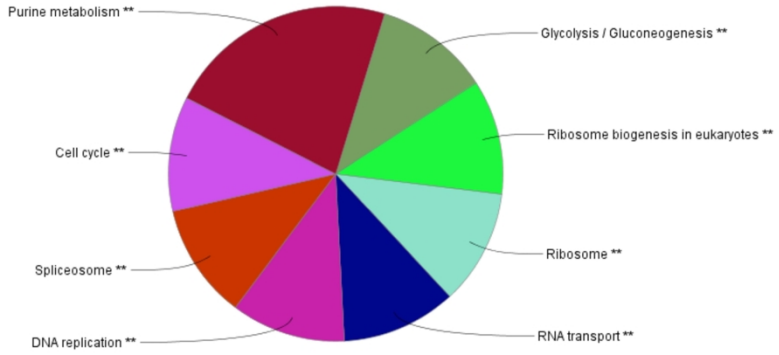

B

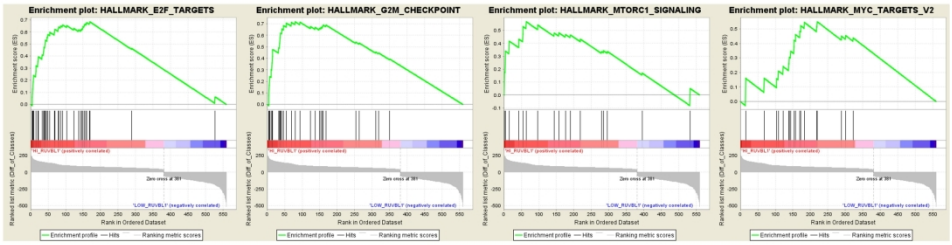

C

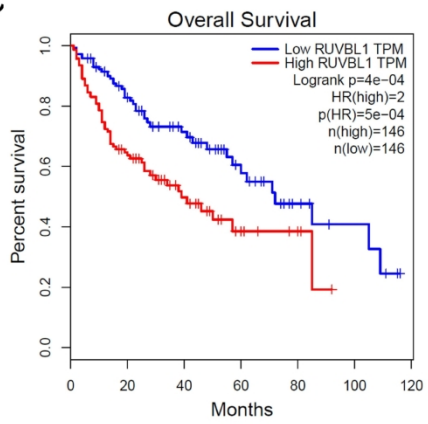

D